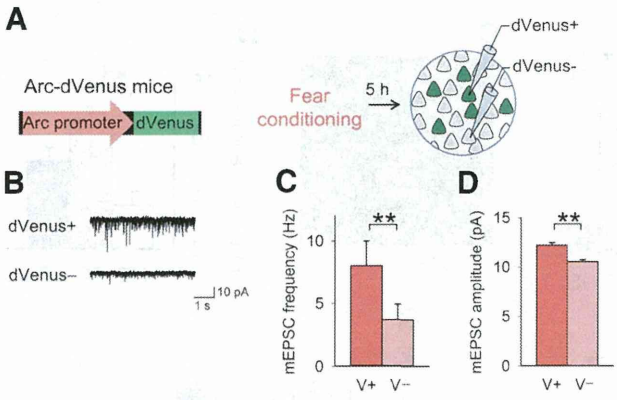

Figure 2. Enhanced synaptic efficacy in the BLA neurons recruited into a fear memory trace is due to fear conditioning but not fear memory retrieval. ***A***, Experimental procedure. ***B***, Representative mEPSC traces recorded from dVenus+ and dVenus− neurons. ***C***, ***D***, dVenus+ neurons had a higher mEPSC frequency (***C***) and amplitude (***D***) than dVenus− neurons ($n = 6$ dVenus+ and 6 dVenus− neurons from 5 mice; frequency, paired t test, $t_{(5)} = 5.4$, $p = 0.0029$; amplitude, $t_{(5)} = 7.8$, $p = 0.00056$); $^{**}p < 0.01$.

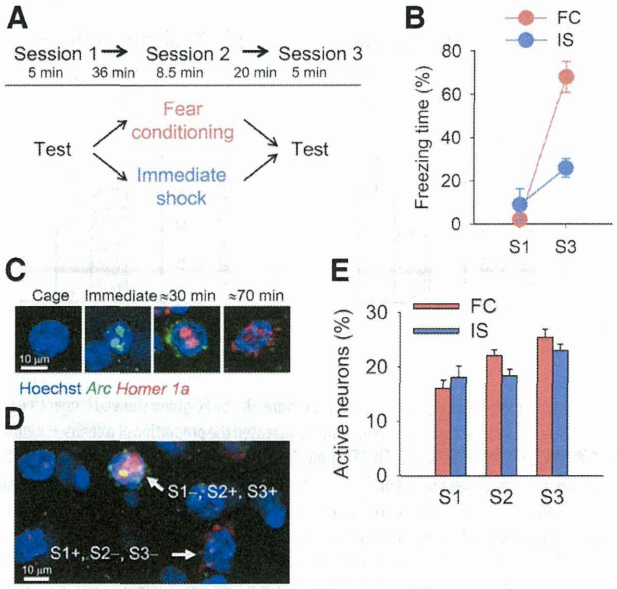

Figure 3. Large-scale activity imaging before, during, and after fear conditioning in the BLA. ***A***, Experimental procedure ($n = 8$ mice per group). ***B***, The FC but not the IS group exhibited contextual conditioned fear in session 3 (repeated-measures ANOVA, $F_{(1,14)} = 23.8$, $p = 0.00025$; FC vs IS in session 3, $p = 0.00017$). ***C***, Representative images of individual BLA neurons from fluorescent *in situ* hybridization of *Arc* and *Homer 1a*. ***D***, A representative image of *Arc* and *Homer 1a* RNA expression from the FC group. A neuron with nuclear and cytoplasmic *Arc* and nuclear *Homer 1a* was activated in sessions 2 and 3 (S1−, S2+, S3+). A neuron with only cytoplasmic *Homer 1a* was activated in session 1 (S1+, S2−, S3−). ***E***, Percentage of BLA neurons active in each session was comparable between the FC and IS groups ($n = 319.0 \pm 18.1$ neurons in FC group and 313.3 ± 17.6 neurons in IS group per mouse).

with 0 and 25 min ($p = 0.00052$ and 0.0013, respectively). Therefore, in the following analysis, we identified neurons that were activated during session 1 (~70 min before being killed), session 2 (~30 min before being killed), and session 3 (immediately before being killed) based on the "cytoplasmic *Homer 1a*," "nuclear *Homer 1a* and cytoplasmic *Arc*," and "nuclear *Arc*," respectively (Fig. 3*C*,*D*). We measured the proportions of active neurons in the BLA during sessions 1, 2, and 3 (Fig. 3*D*). There was no group effect or group × session interaction (Fig. 3*E*).

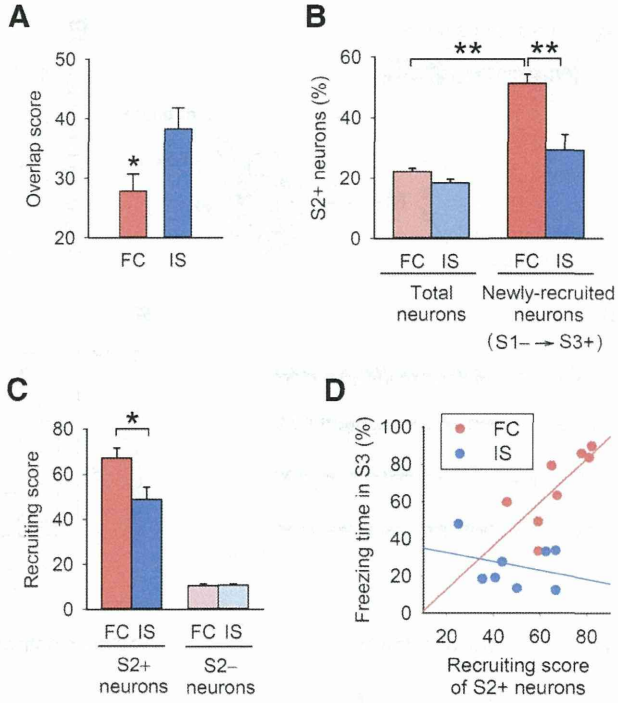

Figure 4. Fear conditioning alters a context-responsive BLA neuronal ensemble based on the neuronal activity during fear conditioning. ***A***, BLA neurons that were active in session 3 overlapped less with those that were active in session 1 in the FC group compared with the IS group (Student's t test, $t_{(14)} = 2.3$, $p = 0.039$). ***B***, BLA neurons newly recruited into the context-responsive ensemble displayed preferential activity in session 2 depending on fear learning (repeated-measures ANOVA, $F_{(1,14)} = 11.0$, $p = 0.0051$; total vs newly recruited neurons in the FC group, $p = 1.5 \times 10^{-5}$). ***C***, The activities of individual BLA neurons during fear conditioning predicted their recruitment into the context-responsive ensemble ($F_{(1,14)} = 7.08$, $p = 0.019$; S2+ (FC) vs S2− (FC), $p = 0.00062$; S2+ (FC) vs S2+ (IS), $p = 0.021$). ***D***, The recruiting effect of activity during fear conditioning in the BLA correlated with the strength of fear memory expression (Pearson's correlation coefficient, $r = 0.74$, $t_{(7)} = 2.7$, $p = 0.036$; Z-test, FC vs IS, $z = 2.0$, $p = 0.023$); $^{**}p < 0.01$, $^{*}p < 0.05$.

To determine whether fear conditioning alters the context-responsive neuronal ensemble, the overlap between the neuronal populations that were active during sessions 1 and 3 was examined. The overlap score of the FC group was lower than that of the IS group (Fig. 4*A*). This result indicates that fear conditioning alters the context-responsive neuronal ensemble.

We further hypothesized that the newly recruited neurons were preferentially activated during conditioning, because synaptic potentiation was observed in neurons that were activated during conditioning. To test this, we measured the percentage of neurons that were active during session 2 (S2+) among the total BLA neurons and among the newly recruited neurons. In the FC group, the S2+ percentage in the newly recruited neurons was higher than that in the total BLA neurons (Fig. 4*B*). In the IS group, on the other hand, there was no significant difference.

To determine whether neurons activated during fear conditioning are newly recruited into the context-responsive ensemble, we calculated a recruiting score consisting of the percentage of S2+ or S2− neurons that changed their activity from inactive in session 1 to active in session 3. In the FC group, the recruiting score of the S2+ neurons was higher than that of the S2− neurons (Fig. 4*C*). Further analysis also indicated that the recruiting effect of session 2 activity was associated with fear conditioning: First, the recruiting score of S2+ neurons of the FC group was higher than that of the IS group (Fig. 4*C*); second, the recruiting

score in the FC group correlated positively with the freezing time in session 3 (Fig. 4*D*). Together, these results indicate that fear conditioning alters the context-responsive neuronal ensemble depending on the neuronal activity during fear conditioning.

Discussion

We demonstrated that contextual fear conditioning induces presynaptic potentiation in cortical, but not thalamic, synapses on BLA neurons that were recruited into the fear memory trace. In accordance with the hypothesis that synaptic modification in a subset of neurons is likely to lead to a reorganization of neuronal ensembles, we also found that fear conditioning alters a context-responsive neuronal ensemble depending on the neuronal activity during fear conditioning. The recruiting effect of activity during fear conditioning correlated with the strength of fear memory expression. Overall, these data suggest that synaptic plasticity in a subset of BLA neurons is likely to contribute to fear memory expression through ensemble reorganization.

A novel finding of this study is that synaptic potentiation associated with learning occurs specifically in neurons that are recruited into the memory trace. Although previous studies showed that fear conditioning induces synaptic potentiation in the BLA synapses (McKernan and Shinnick-Gallagher, 1997; Tsvetkov et al., 2002), it is unclear whether fear conditioning induces synaptic modification of the amygdala globally or only in a subset of neurons. In this study, we challenged this issue by measuring synaptic efficacy from neurons recruited into a memory trace, which are labeled with *Arc* promoter-driven dVenus. We found that presynaptic potentiation is specifically induced in the recruited neurons (dVenus+ neurons). The observed increase in mEPSC frequency in dVenus+ neurons from conditioned mice reflects modifications in whole neurons, whereas the decrease in the PPR was limited to the cortical pathway alone. This might be due to the greater influence of cortical inputs on BLA neurons relative to other inputs. Our findings do not rule out postsynaptic plasticity (Rumpel et al., 2005; Zhou et al., 2009) as another mechanism for contextual fear conditioning. The amplitude of mEPSCs in the dVenus+ neurons was higher compared with dVenus− neurons, but there was no group × dVenus interaction. The postsynaptic enhancement effect of fear conditioning might be masked by footshock stress, which was also given to the IS group.

The activity of individual neurons during learning is likely to determine their recruitment into the memory trace. In this study, we used large-scale activity mapping with the immediate-early genes *Arc* and *Homer 1a* to determine how contextual fear conditioning alters BLA neuronal ensembles. Remarkably, we measured the activities of >300 neurons per mouse separately over three sessions by analyzing subcellular distributions of *Arc* and *Homer 1a* RNA. In doing so, we found that the neurons activated during memory retrieval were preferentially activated during preceding fear conditioning, and the neurons that were activated during fear conditioning were also preferentially activated during memory retrieval. The importance of neuronal activity during learning in recruitment is supported by previous studies using CREB transfection. CREB transfection upregulates excitability of transfected neurons (Zhou et al., 2009) and increases the recruitment ratio of those neurons into a fear memory trace (Han et al., 2007).Together, these findings suggest that the recruitment of neurons into a memory trace is defined by the activity of individual neurons during learning.

In conclusion, we have demonstrated that presynaptic potentiation occurs specifically in neurons that are recruited into a fear memory trace. This synaptic plasticity likely contributes to the ensemble reorganization, an event that positively correlated with the strength of fear memory expression. Together, our findings suggest that synaptic plasticity in a subset of BLA neurons contributes to fear memory expression through the reorganization of a context-responsive neuronal ensemble.

References

Eguchi M, Yamaguchi S (2009) In vivo and in vitro visualization of gene expression dynamics over extensive areas of the brain. Neuroimage 44:1274–1283. CrossRef Medline

Fanselow MS, Kim JJ (1994) Acquisition of contextual Pavlovian fear conditioning is blocked by application of an NMDA receptor antagonist D,L-2-amino-5-phosphonovaleric acid to the basolateral amygdala. Behav Neurosci 108:210–212. CrossRef Medline

Guzowski JF, McNaughton BL, Barnes CA, Worley PF (1999) Environment-specific expression of the immediate-early gene Arc in hippocampal neuronal ensembles. Nat Neurosci 2:1120–1124. CrossRef Medline

Han JH, Kushner SA, Yiu AP, Cole CJ, Matynia A, Brown RA, Neve RL, Guzowski JF, Silva AJ, Josselyn SA (2007) Neuronal competition and selection during memory formation. Science 316:457–460. CrossRef Medline

Han JH, Kushner SA, Yiu AP, Hsiang HL, Buch T, Waisman A, Bontempi B, Neve RL, Frankland PW, Josselyn SA (2009) Selective erasure of a fear memory. Science 323:1492–1496. CrossRef Medline

Hashikawa K, Matsuki N, Nomura H (2011) Preferential arc transcription at rest in the active ensemble during associative learning. Neurobiol Learn Mem 95:498–504. CrossRef Medline

Li XB, Inoue T, Nakagawa S, Koyama T (2004) Effect of mediodorsal thalamic nucleus lesion on contextual fear conditioning in rats. Brain Res 1008:261–272. CrossRef Medline

Maren S (2001) Neurobiology of Pavlovian fear conditioning. Annu Rev Neurosci 24:897–931. CrossRef Medline

Maren S, Fanselow MS (1997) Electrolytic lesions of the fimbria/fornix, dorsal hippocampus, or entorhinal cortex produce anterograde deficits in contextual fear conditioning in rats. Neurobiol Learn Mem 67:142–149. CrossRef Medline

Marrone DF, Schaner MJ, McNaughton BL, Worley PF, Barnes CA (2008) Immediate-early gene expression at rest recapitulates recent experience. J Neurosci 28:1030–1033. CrossRef Medline

McKernan MG, Shinnick-Gallagher P (1997) Fear conditioning induces a lasting potentiation of synaptic currents in vitro. Nature 390:607–611. CrossRef Medline

Miura Y, Naka M, Matsuki N, Nomura H (2012) Differential calcium dependence in basal and forskolin-potentiated spontaneous transmitter release in basolateral amygdala neurons. Neurosci Lett 529:1–6. CrossRef Medline

Nomura H, Matsuki N (2008) Ethanol enhances reactivated fear memories. Neuropsychopharmacology 33:2912–2921. CrossRef Medline

Nomura H, Nonaka A, Imamura N, Hashikawa K, Matsuki N (2012) Memory coding in plastic neuronal subpopulations within the amygdala. Neuroimage 60:153–161. CrossRef Medline

Reijmers LG, Perkins BL, Matsuo N, Mayford M (2007) Localization of a stable neural correlate of associative memory. Science 317:1230–1233. CrossRef Medline

Rumpel S, LeDoux J, Zador A, Malinow R (2005) Postsynaptic receptor trafficking underlying a form of associative learning. Science 308:83–88. CrossRef Medline

Sacchetti B, Lorenzini CA, Baldi E, Tassoni G, Bucherelli C (1999) Auditory thalamus, dorsal hippocampus, basolateral amygdala, and perirhinal cortex role in the consolidation of conditioned freezing to context and to acoustic conditioned stimulus in the rat. J Neurosci 19:9570–9578. Medline

Tsvetkov E, Carlezon WA, Benes FM, Kandel ER, Bolshakov VY (2002) Fear conditioning occludes LTP-induced presynaptic enhancement of synaptic transmission in the cortical pathway to the lateral amygdala. Neuron 34:289–300. CrossRef Medline

Zhou Y, Won J, Karlsson MG, Zhou M, Rogerson T, Balaji J, Neve R, Poirazi P, Silva AJ (2009) CREB regulates excitability and the allocation of memory to subsets of neurons in the amygdala. Nat Neurosci 12:1438–1443. CrossRef Medline

Sound-induced hyperpolarization of hippocampal neurons

Reimi Abe[a,*], Tetsuya Sakaguchi[a,*], Nobuyoshi Matsumoto[a], Norio Matsuki[a] and Yuji Ikegaya[a,b]

The hippocampus is involved in episodic memory, which is composed of subjective experiences in the multisensory world; however, little is known about the subthreshold membrane potential responses of individual hippocampal neurons to sensory stimuli. Using in-vivo whole-cell patch-clamp recordings from hippocampal CA1 neurons in awake mice, we found that almost all hippocampal neurons exhibited a hyperpolarization of 1–2 mV immediately after the onset of a sound. This large-scale hyperpolarization was unaffected by the duration or pitch of the tone. The response was abolished by general anesthesia and a surgical fimbria–fornix lesion. *NeuroReport* 25:1013–1017 © 2014 Wolters Kluwer Health | Lippincott Williams & Wilkins.

NeuroReport 2014, 25:1013–1017

Keywords: hippocampus, inhibitory postsynaptic potential, auditory response, tone

[a]Laboratory of Chemical Pharmacology, Graduate School of Pharmaceutical Sciences, The University of Tokyo, Tokyo and [b]Center for Information and Neural Networks, National Institute of Information and Communication Technology, Osaka, Japan

Correspondence to Yuji Ikegaya, PhD, Laboratory of Chemical Pharmacology, Graduate School of Pharmaceutical Sciences, the University of Tokyo, 7-3-1 Hongo, Bunkyo-ku, Tokyo 113 0033, Japan
Tel: +81 3 5841 4783; fax: +81 3 5841 4786;
e-mail: ikegaya@mol.f.u-tokyo.ac.jp

*Reimi Abe and Tetsuya Sakaguchi contributed equally to the writing of this article.

Received 2 March 2014 **accepted** 13 May 2014

Introduction

The hippocampus plays a role in encoding snapshots during daily life experiences and creating episodic memory [1]. In the rodent, hippocampal neurons modulate their firing patterns depending on the location of the animal and collectively generate a cognitive map of space [2]. Such internal representations regarding behavioral experience emerge and are updated through visual, auditory, olfactory, gustatory, and somatosensory information. Therefore, knowing how hippocampal neurons respond to sensory stimuli is critical; however, the current evidence is contradictory. A classical study using single unit recordings from awake paralyzed rats reported that 41% of the hippocampal neurons decreased their firing rates in response to light, sound, and touch [3]. By contrast, single unit recordings during behavioral tasks or sleep revealed that hippocampal neurons discharged in response to auditory stimuli only when rats had previously been conditioned to the sound [4,5].

Information on the intracellular membrane potential responses of hippocampal neurons to sensory inputs is still sparse, and to the best of our knowledge, those previous studies were all conducted under anesthesia. In urethane-anesthetized rats, for example, hippocampal CA1 neurons exhibit a hyperpolarization in response to somatosensory stimuli [6,7] and θ-rhythm membrane potential fluctuations after tail-pinch stimulation [6]. Importantly, a recent elegant study using functional optical imaging of the hippocampus demonstrated that only awake mice show the activation of septal GABAergic axon fibers in response to sensory stimuli [8]. Therefore, nonanesthetized animals are required to evaluate the true membrane voltage dynamics. In the present work, we patch-clamped hippocampal CA1 neurons in awake, head-restricted mice. We report here that almost all hippocampal neurons respond to auditory and whisker stimulation with a brief hyperpolarization.

Methods

Animals

The experiments were performed with the approval of the animal experiment ethics committee at the University of Tokyo (approval number: P26-5) and according to the NIH guidelines for the care and use of animals. Male ICR mice (21–33 days old) were purchased and housed in cages under standard laboratory conditions (12 h light/dark cycle).

Surgery

Mice were anesthetized with ketamine (50 mg/kg, intraperitoneal) and xylazine (10 mg/kg, intraperitoneal) and were implanted with a metal head-holding plate. After 2 days of recovery, the mice were subjected to head-fixation training on a custom-made, stereotaxic fixture. Training was repeated for 1–3 h/day until the implanted animal learned to remain quiet. During and after each session, the animal was rewarded with free access to sucrose-containing water. Full habituation usually required 5–10 consecutive days. Then, the mice were anesthetized with a ketamine/xylazine cocktail and were craniotomized (1×1 mm^2), centered at 2.2 mm posterior and 2.0 mm lateral to the bregma. The dura was surgically removed, and the exposed brain tissue surface was covered with 1.7% agar. Throughout the experiments, a heating pad maintained the rectal temperature at 37°C, and the surgical region was analgesized with 0.2%

0959-4965 © 2014 Wolters Kluwer Health | Lippincott Williams & Wilkins

DOI: 10.1097/WNR.0000000000000206

Fig. 1

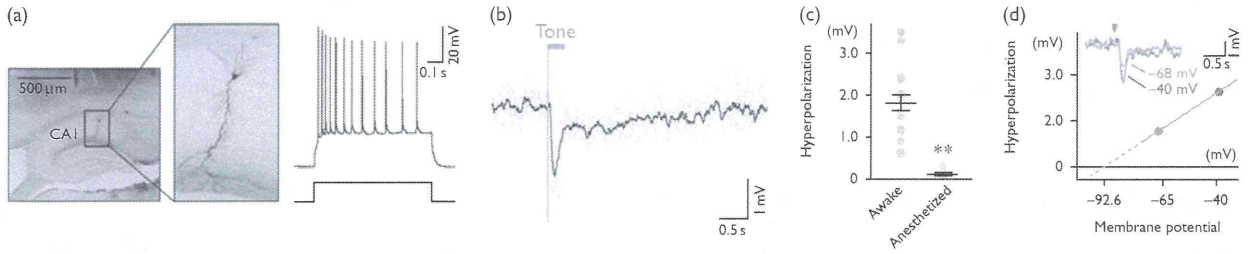

Tone-induced hyperpolarization of hippocampal CA1 neurons. (a) Biocytin reconstruction of an in-vivo, whole-cell recorded CA1 pyramidal cell. The right trace indicates a membrane response to a 200-pA, 1-s current injection (bottom line), showing the regular spiking properties typical of pyramidal cells. (b) The mean membrane potential fluctuations in response to a sound stimulus (green bar, 300 ms, 4 kHz, 110 dB). Gray and black lines indicate the average of seven individual cells across 20 tone-stimulus trials and the average across the seven cells, respectively. (c) No hyperpolarization under urethane anesthesia. Data are represented as mean ± SEMs of 22 cells from 20 awake mice and seven cells from three anesthetized mice. Each dot indicates a single cell. $^{**}P = 4.8 \times 10^{-5}$, $t_{27} = 4.83$, Student's *t*-test. (d) Representative estimation of the reversal potentials of tone-induced hyperpolarization. The experiments were repeated in three mice, producing similar results.

lidocaine. After the mice recovered from the anesthesia, recordings were made under head fixation in a sound-proof box. The experiments shown in Fig. 1c were conducted under anesthesia with urethane (2.0–2.2 g/kg, intraperitoneal). In the experiments shown in Fig. 3, the fimbria–fornix (FF) was bilaterally transected before recording. A retractable knife (4 mm in width) was lowered to ~3 mm deep from the cortex surface through a small burr hole in the skull (0.5 mm posterior, ±2 mm lateral to the bregma) under stereotactic guidance.

Electrophysiology

Patch-clamp recordings were obtained from neurons in the CA1 stratum pyramidale using borosilicate glass electrodes (4–7 MΩ). Pyramidal cells were identified by their regular spiking properties and by post-hoc histological analysis (Fig. 1a). The intrapipette solution consisted of the following (in mM) reagents: 120 K-gluconate, 10 KCl, 10 HEPES, 10 creatine phosphate, 4 MgATP, 0.3 Na_2GTP, 0.2 EGTA (pH 7.3), and 0.2% biocytin. Neurons were sealed at more than 8 GΩ before the whole-cell current-clamp configuration was acquired. To ensure the recording quality, neurons were selected based on their membrane properties with the resting potential ranging between −55 and −75 mV and the input membrane resistance ranging between 35 and 95 MΩ. Experiments in which the series resistance exceeded 70 MΩ or changed by more than 15% during the entire recording session were also discarded.

The data were analyzed offline using custom-made MATLAB (R2012b, Natick, Massachusetts, USA) routines. As auditory stimuli, sine-wave pure tones (duration: 0.03–3 s; frequency: 1–16 kHz; intensity: 70–110 dB) were applied at an interval of 6–8 s from a speaker placed in front of the mice (25 cm away from the nose). In each block, tones with different conditions were presented in a random order. An air puff was applied for 200 ms through a small glass tube to move all the whiskers contralateral to the recording side.

Histology

After each recording, the recording pipette was carefully removed from the brain, and the mice were anesthetized by an overdose of urethane. After they were completely anesthetized, they were perfused transcardially with chilled PBS, followed by 4% paraformaldehyde in 0.1 M PBS (pH 7.4). The brains were carefully removed and stored overnight at 4°C in a 4% paraformaldehyde solution. Then they were sagittally sectioned at a thickness of 100 µm. The sections were incubated with 0.3% H_2O_2 for 30 min. After permeabilization in 0.2% Triton X-100 for 1 h, they were processed with ABC reagent at 4°C overnight and with 0.0003% H_2O_2, 0.02% diaminobenzidine, and 10 mM $(NH_4)_2Ni(SO_4)_2$.

Results

Tone-induced hyperpolarization of hippocampal CA1 neurons

Pyramidal cells were patch-clamped from the CA1 area of awake, head-fixed mice (Fig. 1a). Unless otherwise specified, 4-kHz sine-wave pure tones at 110 dB were applied for 300 ms at intervals of 6–8 s.

Under the $I = 0$ current-clamped configuration, neurons exhibited a rapid membrane potential hyperpolarization in response to a tone, which returned slowly to the baseline within seconds (Fig. 1b). The hyperpolarization was consistently observed for all trials in all neurons recorded, but it did not occur in urethane-anesthetized mice (Fig. 1c). The mean peak amplitude of the hypolarization was 1.8 ± 0.2 mV (Fig. 1c), and the peak latency was 122 ± 8 ms after the tone onset (mean ± SEM of 22 neurons from 20 mice). We also obtained five whole-ce recordings from dentate granule cells. In all five cases, we observed tone-induced hyperpolarizations; the peak

amplitude and latency were 3.3 ± 0.5 mV and 112 ± 15 ms, respectively ($n = 5$ cells from five mice). Therefore, virtually all principal cells in the hippocampal formation appeared to hyperpolarize *en masse* in response to sound.

When CA1 neurons were depolarized to approximately −40 mV by a small direct current injection, the hyperpolarizing response increased in size. The reversal potential was estimated to be approximately −90 mV, close to the reversal potential of GABA receptor-mediated currents (Fig. 1d) ($n = 3$ cells). We analyzed the waveforms of tone-induced hyperpolarizations. The rise time (10–90%) of the hyperpolarizations was 20.4 ± 2.1 ms, and the decay time constant was 64.0 ± 6.6 ms. These kinetics are a few times slower than single-pulse stimulation-evoked phasic GABAergic inhibitory postsynaptic potentials in mouse CA1 pyramidal cells [9], suggesting that a tone-induced hyperpolarization was produced by a burst of spikes of inhibitory interneurons. Consistent with this idea, we encountered one anecdotal whole-cell recording from the deep CA1 stratum radiatum in which a nonpyramidal neuron (but cell-type unidentified) responded reliably to sound with a burst of spikes; the burst response occurred in all 10 trials with a first-spike latency of 29 ± 1 ms, and each burst consisted of 3.9 ± 0.2 spikes at 181 ± 4 Hz (mean ± SEM of 10 trials).

The hyperpolarizing responses were highly stereotyped; the hyperpolarization amplitude was invariant over the durations and pitches of the tones (Fig. 2a and b), and no apparent OFF responses occurred (data not shown). Therefore, these responses were unlikely to encode the texture of sound.

The hyperpolarization amplitude increased with increased tone intensities (Fig. 2c). Transient hyperpolarizations were also induced by air puff-induced whisker deflection. Their peak amplitude and latency were 1.4 ± 0.3 mV and 122 ± 7 ms, respectively, and were compatible with those of sound-induced hyperpolarizations (Fig. 2d) ($n = 6$ neurons from five mice). Therefore, sound-induced hyperpolarization may reflect sudden whisker movement as a startle response, because the sound pressure that neurons responded to was high. To address this possibility, we monitored the responses of whiskers to auditory stimulation. The significant whisker movement was considered when the maximal deflection angle of the A2 or B2 whisker within 100 ms after the onset of a tone stimulus exceeded 2 × SDs of the spontaneous whisker movements during any given 100-ms period without sound. Of the 360 tone stimuli (4 kHz, 110 dB) applied to three mice, only 58 (16.1%) trials elicited the whisker movement. Therefore, tone-induced whisker movements, if any, cannot fully account for sound-induced hyperpolarizations. Moreover, we examined whether the hyperpolarizing responses are affected by tone prepulses because a weak sound stimulus transiently inhibits a behavioral startle to a closely following strong sound stimulus [10]. A 20-ms prepulse tone with 76 or 85 dB did not reduce the hyperpolarization induced by a 110-dB tone applied 100 ms later (Fig. 2e), although we confirmed that these stimulation conditions readily induced behavioral prepulse inhibition in freely behaving mice (data not shown).

Lack of hippocampal tone responses in fimbria–fornix-lesioned mice

The major afferents to the hippocampus are supplied through the temporoammonic pathway from the entorhinal cortex and the FF pathway from subcortical areas. Medial–septal neurons, which project to the hippocampus through FF fibers, increase their firing rates in response to various sensory stimuli, including sound, touch, and light [11,12]. A recent imaging study demonstrated that medial–septal fibers projecting to CA1 stratum oriens respond to sensory inputs with transient calcium elevations [8,13]. We thus applied tone stimuli to mice in which the FF was surgically transected (Fig. 3a). In these mice, CA1 neurons did not exhibit tone-induced hyperpolarization (Fig. 3b and c).

Fig. 2

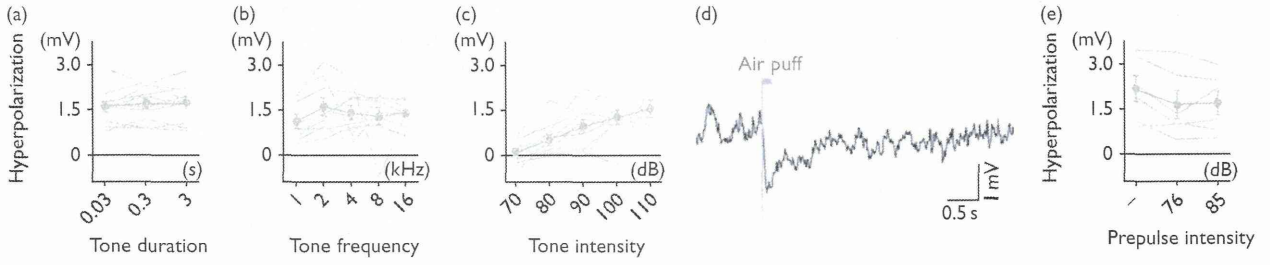

Properties of tone-induced hyperpolarization. (a–c) Dependence of the mean response magnitude on the tone duration [(a) $n = 11$ cells from 11 mice, $P = 0.86$, $F_{2,30} = 0.15$, one-way analysis of variance], the tone pitch [(b) $n = 9$ cells from eight mice, $P = 0.72$, $F_{4,40} = 0.51$], and the tone intensity [(c) $n = 10$ cells from 10 mice, $P = 1.7 \times 10^{-4}$, $F_{4,45} = 7.06$]. (d) The average response to an air puff stimulus (200 ms in duration), $n = 6$ cells from five mice. (e) Small effect of a 20-ms prepulse stimulus (4 kHz, 76 or 85 dB) 100 ms before a loud tone (4 kHz, 110 dB) on the response amplitude to the loud tone, $n = 6$ cells from five mice, $P = 0.65$, $F_{2,15} = 0.43$. Error bars are SEMs.

Fig. 3

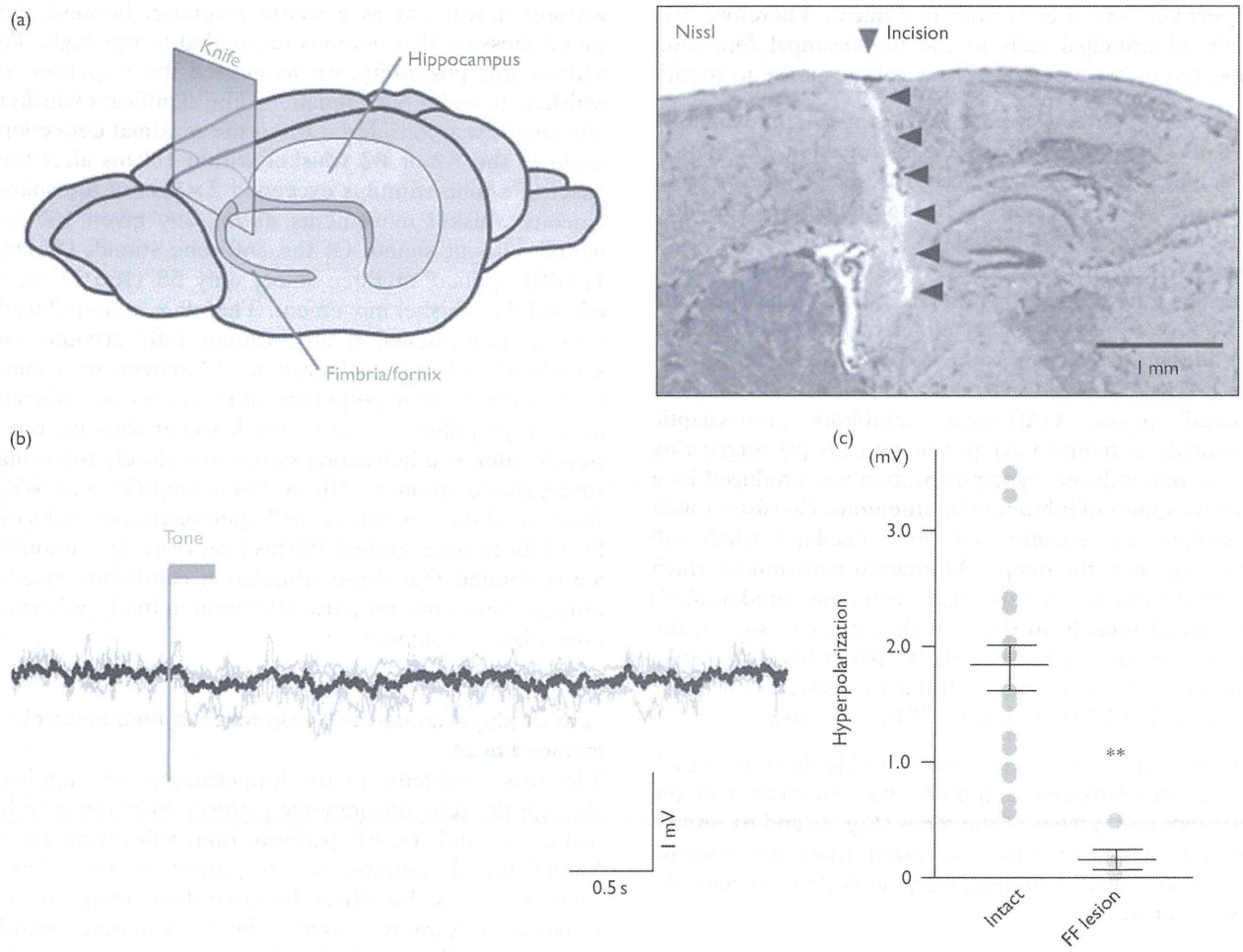

A lack of hippocampal tone responses in fimbria–fornix (FF)-lesioned mice. (a) The FF fibers were surgically transected by lowering a microknife into the subcortical region. (b) The mean voltage responses to tones (0.3 s, 4 kHz, 110 dB) in FF-lesioned mice. Gray and black lines indicate the trial average of five individual cells from five mice and the average across the five cells, respectively. (c) The mean ± SEMs of the tone-induced hyperpolarization magnitude in 22 intact and five FF-lesioned mice. Each dot indicates a single neuron. $^{**}P = 2.6 \times 10^{-4}$ vs. intact, $t_{25} = 3.97$, Student's *t*-test.

Discussion

We demonstrated that in awake mice, CA1 pyramidal cells responded to the onset of a sound and whisker deflection with a transient hyperpolarization. Because we observed the hyperpolarizing responses in all neurons recorded, the responses are likely a large-scale phenomenon that occurs in the entire CA1 network. The hyperpolarization was unaffected by the sound duration, the sound pitch, or brief sound prepulse exposure. The response was abolished by general anesthesia and a surgical FF lesion.

All hippocampal fields receive both excitatory and inhibitory projections through the FF pathway [14]. Because medial–septal neurons fire in response to various sensory stimuli [11,12], the medial septum is a candidate brain area that mediates sound-induced hyperpolarization in the hippocampus. Indeed, hippocampal GABAergic afferents from the medial septum are responsive to auditory stimulation [8]. These fibers are known to terminate on inhibitory interneurons and may disinhibit pyramidal cells. In contrast to this expectation, CA1 pyramidal cells exhibited a transient membrane potential hyperpolarization. In addition to GABAergic projections, however, the medial septum sends cholinergic and glutamatergic fibers to the hippocampus [13,15]. These excitatory inputs may activate hippocampal interneurons and thereby elicit a hippocampal network suppression.

In conclusion, we characterized sensory modulation of hippocampal neurons. This modulation emerged through different afferents from entorhinohippocampal inputs

that are likely to produce place-cell activity [16]. Such information convergences from different neuronal pathways may contribute to the encoding of episodic memory.

Acknowledgements

This work was partly supported by Grants-in-Aid for Science Research on Innovative Areas (22115003; 25119004), the Japan Society for the Promotion of Science through the Funding Program for Next Generation World-Leading Researchers (LS023), and Strategic Research Program for Brain Sciences.

Conflicts of interest

There are no conflicts of interest.

References

1 Scoville WB, Milner B. Loss of recent memory after bilateral hippocampal lesions. *J Neurol Neurosurg Psychiatry* 1957; **20**:11–21.
2 O'Keefe J, Dostrovsky J. The hippocampus as a spatial map. Preliminary evidence from unit activity in the freely-moving rat. *Brain Res* 1971; **34**:171–175.
3 Miller SW, Groves PM. Sensory evoked neuronal activity in the hippocampus before and after lesions of the medial septal nuclei. *Physiol Behav* 1977; **18**:141–146.
4 Vinnik E, Antopolskiy S, Itskov PM, Diamond ME. Auditory stimuli elicit hippocampal neuronal responses during sleep. *Front Syst Neurosci* 2012; **6**:49.
5 Itskov PM, Vinnik E, Honey C, Schnupp J, Diamond ME. Sound sensitivity of neurons in rat hippocampus during performance of a sound-guided task. *J Neurophysiol* 2012; **107**:1822–1834.
6 Kamondi A, Acsády L, Wang XJ, Buzsáki G. Theta oscillations in somata and dendrites of hippocampal pyramidal cells in vivo: activity-dependent phase-precession of action potentials. *Hippocampus* 1998; **8**:244–261.
7 Bellistri E, Aguilar J, Brotons-Mas JR, Foffani G, de la Prida LM. Basic properties of somatosensory-evoked responses in the dorsal hippocampus of the rat. *J Physiol* 2013; **591**:2667–2686.
8 Kaifosh P, Lovett-Barron M, Turi GF, Reardon TR, Losonczy A. Septo-hippocampal GABAergic signaling across multiple modalities in awake mice. *Nat Neurosci* 2013; **16**:1182–1184.
9 Kehrer C, Dugladze T, Maziashvili N, Wojtowicz A, Schmitz D, Heinemann U, Gloveli T. Increased inhibitory input to CA1 pyramidal cells alters hippocampal gamma frequency oscillations in the MK-801 model of acute psychosis. *Neurobiol Dis* 2007; **25**:545–552.
10 Hoffman HS, Ison JR. Reflex modification in the domain of startle: I. Some empirical findings and their implications for how the nervous system processes sensory input. *Psychol Rev* 1980; **87**:175–189.
11 Mercer LF Jr, Remley NR. Mapping of sensory-responsive cells in the septal area of the rat. *Brain Res Bull* 1979; **4**:483–490.
12 Zhang H, Lin SC, Nicolelis MA. A distinctive subpopulation of medial septal slow-firing neurons promote hippocampal activation and theta oscillations. *J Neurophysiol* 2011; **106**:2749–2763.
13 Lovett-Barron M, Kaifosh P, Kheirbek MA, Danielson N, Zaremba JD, Reardon TR, *et al.* Dendritic inhibition in the hippocampus supports fear learning. *Science* 2014; **343**:857–863.
14 Carre GP, Harley CW. Glutamatergic activation of the medial septum complex: an enhancement of the dentate gyrus population spike and accompanying EEG and unit changes. *Brain Res* 2000; **861**:16–25.
15 Amaral D, Lavanex P. Hippocampal neuroanatomy. In: Andersen PMR, Amaral D, Bliss T, O'Keefe J, editors. *The hippocampus book.* Oxford, New York: Oxford University Press; 2007. pp. 37–114.
16 Brun VH, Otnass MK, Molden S, Steffenach HA, Witter MP, Moser MB, Moser EI. Place cells and place recognition maintained by direct entorhinal-hippocampal circuitry. *Science* 2002; **296**:2243–2246.

Onoue et al. Molecular Brain 2014, 7:30
http://www.molecularbrain.com/content/7/1/30

Molecular Brain

SHORT REPORT Open Access

Fear extinction requires Arc/Arg3.1 expression in the basolateral amygdala

Kousuke Onoue[1†], Daisuke Nakayama[1†], Yuji Ikegaya[1,2], Norio Matsuki[1] and Hiroshi Nomura[1*]

Abstract

Background: Prolonged re-exposure to a fear-eliciting cue in the absence of an aversive event extinguishes the fear response to the cue, and has been clinically used as an exposure therapy. Arc (also known as Arg3.1) is implicated in synaptic and experience-dependent plasticity. Arc is regulated by the transcription factor cAMP response element binding protein, which is upregulated with and necessary for fear extinction. Because Arc expression is also activated with fear extinction, we hypothesized that Arc expression is required for fear extinction.

Findings: Extinction training increased the proportion of Arc-labeled cells in the basolateral amygdala (BLA). *Arc* was transcribed during latter part of extinction training, which is possibly associated with fear extinction, as well as former part of extinction training. Intra-BLA infusions of *Arc* antisense oligodeoxynucleotide (ODN) before extinction training impaired long-term but not short-term extinction memory. Intra-BLA infusions of *Arc* antisense ODN 3 h after extinction training had no effect on fear extinction.

Conclusion: Our findings demonstrate that Arc is required for long-term extinction of conditioned fear and contribute to the understanding of extinction as a therapeutic manner.

Keywords: Arc/Arg3.1, Fear conditioning, Extinction, Amygdala

Findings

Background

Excessive fear is related to the pathogenesis of psychiatric disorders such as post-traumatic stress disorder. Prolonged re-exposure to a fear-eliciting cue in the absence of aversive events reduces the fear response to the cue, and has been clinically used as an exposure therapy. De novo gene expression contributes to the consolidation of fear extinction. In fact, activation of the transcription factor cAMP response element binding protein (CREB) increases with fear extinction, and its blockade impairs fear extinction [1]. Inhibition of protein synthesis also impairs fear extinction [2].

Reduction of synaptic strength is proposed as a cellular mechanism for fear extinction [3], which is accompanied by reduced firing of amygdala neurons [4] and a decrease in the surface expression of α-amino-3-hydroxy-5-methyl-4-isoxazolepropionic acid receptors (AMPARs) [5]. These mechanisms are supported by experiments demonstrating that the disruption of AMPAR endocytosis impairs fear extinction [5,6].

The activity-regulated cytoskeletal-associated protein (Arc, also known as Arg3.1) is transcribed during robust neural activity [7,8] and is involved in the inhibition of synaptic strength [9]. Increased expression of Arc reduces AMPAR-mediated synaptic transmission by accelerating receptor endocytosis [10,11]. *Arc* transcription is regulated by CREB [12], which is upregulated with and necessary for fear extinction [1]. Because Arc expression is also activated with fear extinction [1], we hypothesized that Arc expression would be required for fear extinction. We chose the basolateral amygdala (BLA) as a target region because gene expression here is essential for fear extinction [1]. In this study, we tested whether Arc expression in the BLA is required for extinction of contextual conditioned fear.

* Correspondence: nomura@mol.f.u-tokyo.ac.jp
†Equal contributors
[1]Laboratory of Chemical Pharmacology, Graduate School of Pharmaceutical Sciences, The University of Tokyo, 7-3-1 Hongo, Bunkyo-ku, Tokyo 113-0033, Japan
Full list of author information is available at the end of the article

Results

Arc expression is upregulated in the BLA after extinction training

In the first experiment, we tested whether extinction training upregulates Arc expression in the BLA. Mice in the Extinction group underwent contextual fear conditioning, and were subjected to extinction training the next day where they were re-exposed to the conditioning context for 40 min without shock (Experiment 1, Figure 1A). This long-term re-exposure decreased freezing duration over time (0–5 min vs. 35–40 min, $t_{(6)} = 3.6$, $p = 0.016$). Mice were killed 90 min after the extinction training, and their brains were processed immunohistochemically for Arc. Mice in the No Extinction group received contextual fear conditioning similarly to the Extinction group, but without extinction training. The Extinction group demonstrated more Arc-labeled cells relative to the No Extinction group, in both the basal (BA) ($t_{(10)} = 4.3$, $p = 0.0016$) and lateral amygdala (LA) ($t_{(10)} = 4.8$, $p = 0.00069$) (Figure 1B and C).

A previous study reported that even a few minutes of re-exposure to the conditioning context, which induces memory reconsolidation but not fear extinction, upregulates *Arc* expression [1,13]. Thus, greater Arc expression following extinction training might be related to memory reconsolidation but not fear extinction. To distinguish the Arc expression specific to the extinction training from that related to memory reactivation and/or reconsolidation, we utilized *Arc* cellular compartment analysis of temporal activity by fluorescence *in situ* hybridization (catFISH). Transcribed *Arc* RNA first appears in neuronal nuclei, and processed *Arc* mRNA then accumulates in the cytoplasm about 30 min after neural activity. Therefore, an analysis of the subcellular localization of *Arc* enables us to identify active neuronal ensembles during two time points that were separated by a 20–30 min interval. Mice in the Extinction group were re-exposed to the conditioning context for 35 min, and their brain slices were subjected to *Arc* fluorescence *in situ* hybridization (Experiment 2, Figure 2A). The Extinction group demonstrated more cytoplasmic and nuclear *Arc*+ cells relative to the No Extinction group in the basolateral amygdala (cytoplasmic *Arc*, $t_{(12)} = 4.8$, $p = 0.00024$; nuclear *Arc*, $t_{(12)} = 5.2$, $p = 0.00024$); Figure 2B and C). This result indicates that *Arc* transcription is induced during both former and latter parts of extinction training, and the latter part of *Arc* transcription is possibly associated with fear extinction but not memory reconsolidation.

Inhibiting *Arc* translation in the BLA impairs long-term extinction of conditioned fear

To inhibit Arc expression transiently, we employed antisense oligodeoxynucleotide (ODN) approach. By reference to a previous study [14], we designed *Arc* antisense ODN, which significantly decreased Arc levels but did not affect c-Fos or Zif268 levels (Additional file 1). Next, to ask whether Arc expression in the BLA is required for fear extinction, we inhibited Arc expression related to extinction training with the *Arc* antisense ODN. Mice underwent fear conditioning and extinction training (Experiment 4, Figure 3A). They received intra-BLA infusions of an *Arc* antisense or a scrambled ODN 3 h before extinction training (Figure 3C). Overall freezing duration did not differ across groups during extinction training ($F_{(1,\ 26)} = 0.46$, $p = 0.51$), and there was no significant group × time interaction ($F_{(9,\ 234)} = 0.63$, $p = 0.77$). Freezing duration did, however, decrease significantly over time ($F_{(9,\ 234)} = 87.5$, $p = 8.2 \times 10^{-70}$) (Figure 3B). Mice

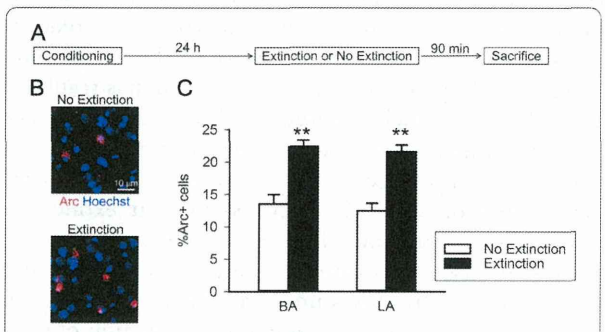

Figure 1 Extinction training upregulates Arc expression in the BLA. (A) The Extinction group underwent contextual fear conditioning and extinction training, in which they were re-exposed to the conditioning context for 40 min without shock. The No Extinction group underwent fear conditioning but not extinction training. **(B)** Representative images of Arc-immunolabeled cells in the Extinction and No Extinction groups, respectively. **(C)** The Extinction group demonstrated more Arc-labeled cells relative to the No Extinction group in both BA and LA (n = 6 mice per group, $^{**}p < 0.01$).

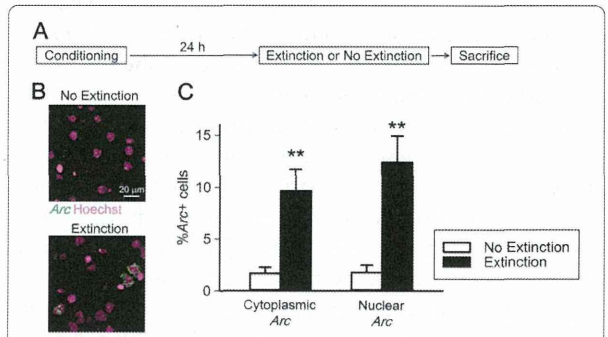

Figure 2 *Arc* is transcribed during both former and latter parts of extinction training. (A) The Extinction group underwent contextual fear conditioning and extinction training, in which they were re-exposed to the conditioning context for 35 min without shock. The No Extinction group underwent fear conditioning but not extinction training. **(B)** Representative images of *Arc*-positive cells in the Extinction and No Extinction groups, respectively. **(C)** The Extinction group demonstrated more cytoplasmic and nuclear *Arc*-positive cells relative to the No Extinction group in the BLA (Extinction, n = 5 mice; No Extinction, n = 9 mice, $^{**}p < 0.01$).

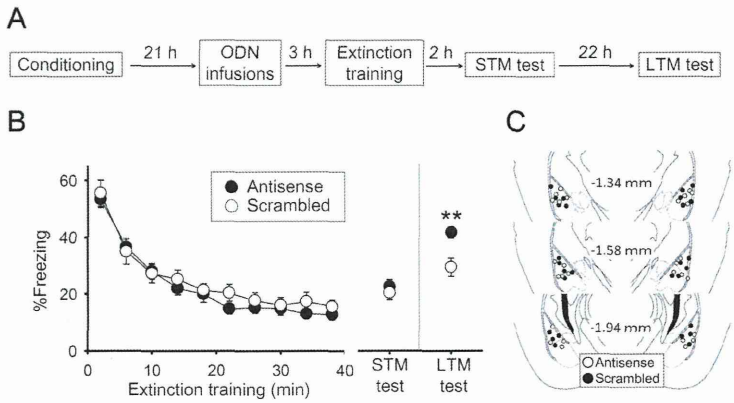

Figure 3 Inhibiting *Arc* translation in the BLA impairs long-term extinction of conditioned fear. (A) Mice received intra-BLA infusions of either *Arc* antisense or scrambled ODN 3 h before extinction training, and were subjected to short-term (STM) and long-term memory (LTM) tests 2 h and 24 h later, respectively. **(B)** Freezing time during extinction training decreased over time. The mice that received antisense ODN had a longer freezing period versus the mice that received scrambled ODN in the LTM test, but not the STM test (n = 14 mice per group, $^{**}p < 0.01$). **(C)** Histological verification of cannula placements for mice infused with *Arc* antisense or scrambled ODN.

were subjected to short-term (STM) and long-term memory (LTM) tests 2 and 24 h later, respectively. Repeated-measures analysis of variance (ANOVA) revealed a significant group × test interaction ($F_{(1,\ 26)} = 4.8$, $p = 0.038$). The mice that received antisense ODN showed longer freezing relative to the mice that received scrambled ODN in the LTM test ($p = 0.0028$) but not the STM test ($p = 0.54$) (Figure 3B). These results indicate that Arc expression is required for long-term extinction of conditioned fear.

Time-limited effect of inhibiting *Arc* translation in the BLA on fear extinction

Finally, we tested whether the effect of inhibiting BLA *Arc* translation on fear extinction depends on the time interval between extinction training and Arc inhibition. Mice were subjected to both fear conditioning and extinction training (Experiment 5, Figure 4A). Freezing duration decreased over time with extinction training (time effect, $F_{(9,\ 216)} = 14.99$, $p = 7.78 \times 10^{-19}$). Mice received intra-BLA infusions of either *Arc* antisense ODN or scrambled ODN 3 h after extinction training (Figure 4C). On the next day, both groups exhibited equivalent periods of freezing ($t_{(24)} = 0.30$, $p = 0.77$) (Figure 4B), suggesting that the effect of inhibiting *Arc* translation in the BLA on fear extinction is time-limited.

Discussion

In this study, we have demonstrated the involvement of Arc in fear extinction. We found that 1) extinction training increased the proportion of Arc-labeled cells in the BLA; 2) *Arc* was transcribed during latter part as well as

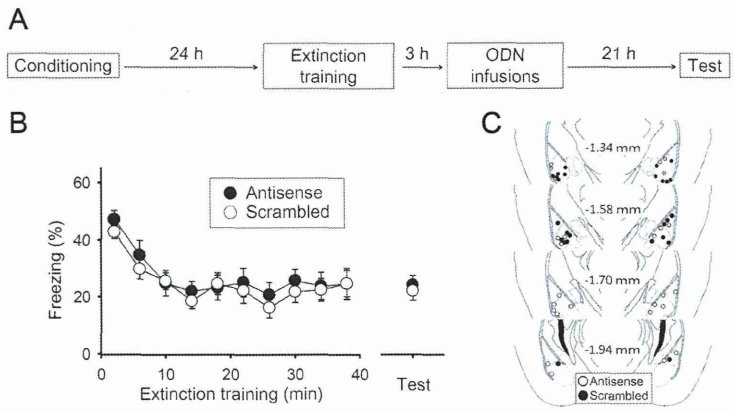

Figure 4 Time-limited effect of inhibiting *Arc* translation in the BLA on fear extinction. (A) Mice received intra-BLA infusions of either *Arc* antisense or scrambled ODN 3 h after extinction training and were given a memory test 24 h later. **(B)** Both groups exhibited equivalent periods of freezing (n = 13 mice per group). **(C)** Histological verification of cannula placements for mice infused with Arc antisense or scrambled ODN.